Layout Optimization of Process Module on Floating Storage and Re-gasification Unit Using QRA

Younghun Kim[1,2], Sung Hee Kim[2], Hyun Joon Nam[2], Woo Hyun Bae[3], In-Beum Lee[4] and Suh-Young Lee[1]

[1] *Department of Chemical Engineering, Pohang University of Science and Technology, 77 Cheongam-ro, Nam-gu, Pohang, Gyeongbuk, 37674, Republic of Korea*
[2] *Korea Shipbuilding & Offshore Engineering Co., Ltd., 75 Yulgok-ro, Jongno-gu, Seoul, 03058, Republic of Korea*
[3] *Hyundai Heavy Industries Co., Ltd., 188 Bangeojinsunhwan-ro, Dong-gu, Ulsan, 682792, Republic of Korea*
[4] *School of Energy & Chemical Engineering, Ulsan National Institute of Science and Technology, Ulsan 44919, Republic of Korea*

Keywords: Process System, Layout Optimization, Operation and Maintenance, Quantitative Risk Assessment

The floating storage regasification unit (FSRU) process has been designed & constructed as modules to achieve the fastest delivery and the easiest installation of an offshore liquefied natural gas (LNG) project. Project efficiencies, including the cost of handling materials, minimization of project delays, and avoidance of bottlenecks require the use of an appropriate module layout in the engineering phase. We present a new framework for the module layout optimization problem in the FSRU process, considering the risk, operation, and maintenance of the process module in a limited area. The developed model aims to minimize the cost of the piping connected between the modules considering both the safety and economy of the process against fire and explosion scenarios. In addition, a quantitative risk assessment (QRA) study was conducted using individual risk indices for determining the risk-avoiding safety distance between the module and the control bridge to evaluate the risk associated with the LNG regasification process. Moreover, a case study was conducted on the conceptual design layout to illustrate the applicability of the proposed model on an FSRU that can process 1,000 million standard cubic feet per day. Overall, the developed model suggested safety guidelines for the operation and maintenance of the optimal module layout in case of fire & explosion accident.

Introduction

Floating storage regasification unit (FSRU) has emerged as the best strategy for succeeding in the liquefied natural gas (LNG) market. The rapidly expanding fleets of FSRUs have equipped the LNG industry with a technically-enhanced set of vessels which has helped FSRUs to penetrate a wide range of gas markets. In particular, a FSRU can deliver regasified LNG to end-user at flow rates ranging from 50 million standard cubic feet per day (MMSCFD) to 750 MMSCFD in highly flexible and cost-effective means as compared to shore-based LNG terminals (Maksym and Wood, 2018). Moreover, the production availability can be satisfied with a more efficient arrangement using 4×33% trains (1000 MMSFCD) that provides greater availability and an improved turn-down flexibility in the market (Songhurst, 2017).

A FSRU is a special type of ship for LNG transfer that essentially use the same technology as onshore LNG terminals, except that the equipment is marinized to be suitable for shipyard construction and marine operation. The FSRU holds several advantages over conventional LNG terminals: (1) cost-effectiveness, (2) time-efficient implementation, (3) environmentally benign as it requires less land and is reusable for linkage with old LNG carriers, and (4) safe. Because off-shore installation usually increases the distance from populated areas.

FSRUs are mainly membrane-type custom-built vessels incorporating an onboard regasification system that vaporizes LNG to deliver high-pressure natural gas (**Figure 1**).

Assuming no under incidents occur during project implementation, the total project schedule of a FSRU should not exceed 30 months (**Figure 2**) including the engineering, constructions and operation tests (Park *et al.*, 2019).

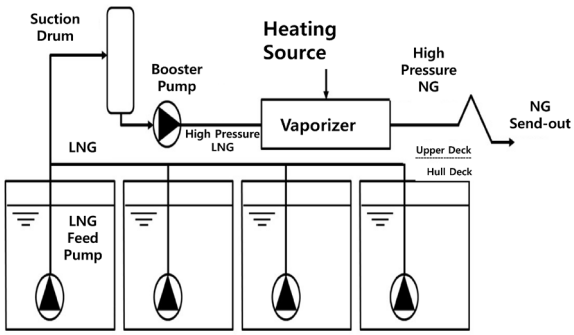

Fig. 1 Schematics of an FSRU (Park *et al.*, 2019)

Received on August 12, 2020; accepted on December 8, 2020
DOI: 10.1252/jcej.20we150
Correspondence concerning this article should be addressed to S.-Y. Lee (E-mail address: suhyoung@postech.ac.kr).

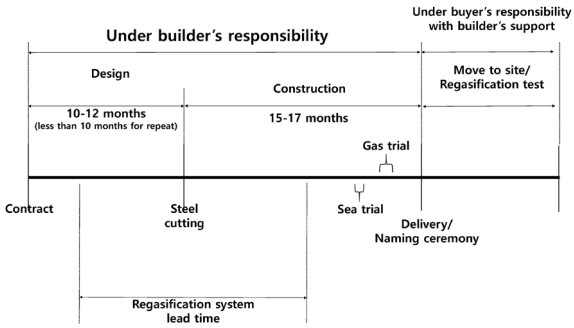

Fig. 2 FSRU project schedule (Park *et al.*, 2019)

The LNG process has been designed and constructed as modules that include unmodifiable elements for planning and realization of assemblies to implement the fastest delivery and the easiest installation of a FSRU project (Kobayashi, 2019). This module comprises necessary equipment that guarantee the performance of the process. Similarly, the layout optimization of the FSRU process module can considering safety and maintenance achieve economical design without any project delay.

Several studies have used mathematical modeling to suggest the optimal layout of a chemical process. Papageorgiou and Rotstein (1998) presented mathematical programming models to obtain the optimal process plant layout assuming rectangular equipment footprints of arbitrary dimensions. Georgiadis *et al.* (1999) developed a multi-floor layout optimization model that includes equipment penetrating more than one floor. Similarly, Patsiatzis *et al.* (2004) proposed a multi-floor chemical plant layout optimization model considering possible accidents and evaluated its financial risk using the Dow Fire and Explosion Index system. Ejeh *et al.* (2019) presented an optimal multi-floor process layout for a LNG plant considering its cost of construction ease of operation and expansion, general safety levels within the plant and its neighboring environment, and operational costs.

Moreover, several scholars have tried to solve the optimal layout problem in the off-shore industry. Ku *et al.* (2014) suggested the optimal equipment layout on a multi-floor LNG liquefaction module for floating liquefied natural gas (FLNG). Furthermore, Jeong *et al.* (2015) proposed an optimal layout solving approach for floating production and storage offloading (FPSO), considering the piping & installation cost of the module and the weight balance.

However, these approaches have limitations to apply directly on layout optimization problems for FSRUs, because they do not consider the modular characteristic of FSRUs and the safety guidelines for the operation and maintenance of an LNG liquefaction process on an offshore structure.

The process modules of FSRUs, including separation, compression, and regasification, are sparsely located on the top-side of the FSRUs, whereas that of a typical FLNG include compact structures of several chemical processing units for separation of gas from oil, gas liquefaction, LNG storage, offloading, and so forth (Park *et al.*, 2018b). However, the FPSO has a similar process configuration to FLNG, except for cryogenic and liquefaction processes. Thus, previous studies of layout optimization of offshore industry on FPSOs or FLNGs have focused on minimizing the piping between the process equipment without overlapping and violating safety regulations. Therefore, the FSRU optimization should focus on minimizing the cost of connecting pipelines between the modules following the safety regulations.

FSRU vessels classified as either ships or offshore installations are under the regulation of international marine safety standards, particularly the LNG trading operation (Songhurst, 2017). International marine safety standards dictate that a ship intended to operate for re-gasification must undergo a fire and explosion risk assessment at the design phase (No, 2014). In addition, decisions regarding the plant layout should consider the economic and safety aspects of the operation as well as management of the target process (Xu and Papageorgiou, 2009). However, there is a limited number of studies on layout optimization that consider systematic fire and explosion risk assessment for process modules and maintenance.

Thus, this study evaluated the risk associated with the LNG regasification process of the FSRU modules by conducting a quantitative risk assessment (QRA) using the event-tree analysis to identify all the potential accident scenarios and sequences in a complex system. In addition, an individual risk (IR) approach based on the QRA study was applied to obtain risk-avoiding safety distance between process modules and the control bridge.

Moreover, the current study considered both the safety and economic aspects of the layout optimization problem to provide a comprehensive method for the optimal layout design of a FSRU in terms of operation and maintenance. Furthermore, several case studies were conducted to evaluate the layout of process modules on the upper deck and the required cost of piping the modules under various process configurations (**Table S1**). This research makes three main contributions:

(1) The proposed model provides a comprehensive strategy for the layout of a FSRU by considering the safety and maintenance of the process module in a limited area.
(2) The QRA study of FSRU based on the individual risk this approach provides information on the safety distance that can mitigate fire and explosion risks between process module and working area.
(3) The suggested case studies investigate the module_module integration effect on the re-gasification process of FSRUs.

1. Methodology of FSRU Layout Optimization

The layout optimization procedure (**Figure 3**) for a FSRU incorporates: (1) a module section, in which we determined its actual size; (2) a safety section, in which safety distances were suggested by considering the results of QRA and noise calculation; (3) an operation and maintenance section, in which the additional constraints were configured to satisfy the rules and requirements of operation and maintenance related to the module placement in a limited area; (4) the

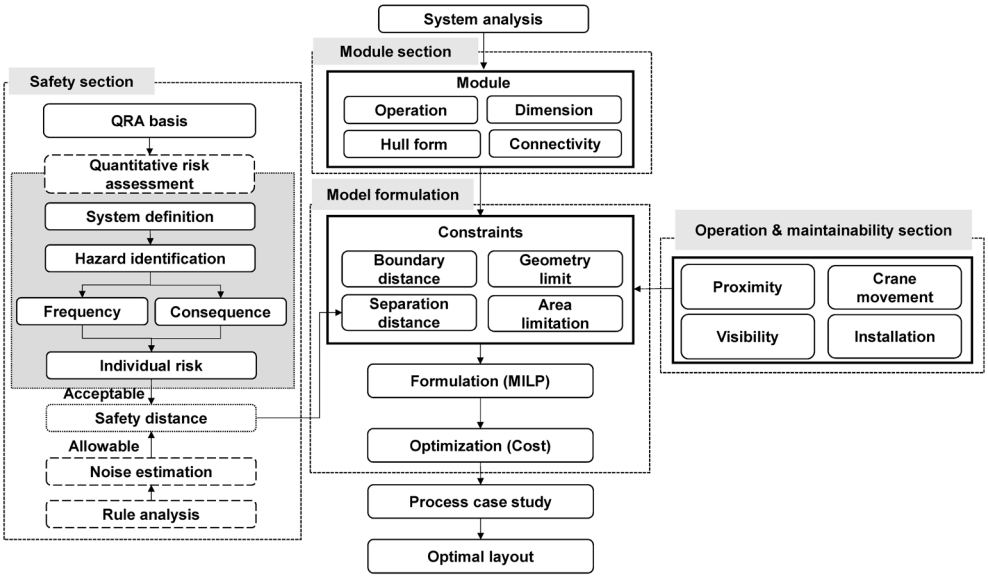

Fig. 3 Procedure for FSRU module layout optimization

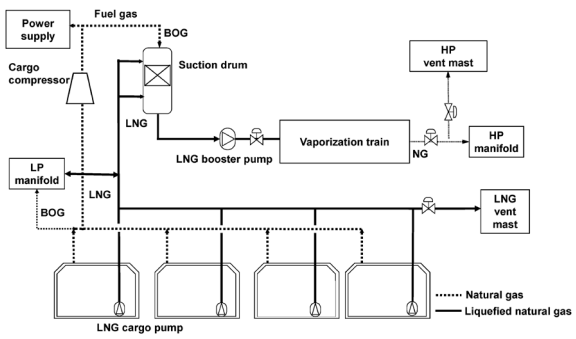

Fig. 4 Typical process flow scheme of FSRU

model formulation, in which the optimal layout results were selected based on the developed mathematical model.

1.1 System analysis

In this study, the layout scope of the FSRU includes the process modules related to the LNG regasification operation. LNG is received through a low pressure (LP) manifold and cooled to approximately −160°C at atmospheric pressure and stored in the membrane tanks (**Figure 4**) (Giardina and Morale, 2015). The cooled LNG is directed to the suction drum from storage tanks through LP pumps (~6 barg) to come in contact with the boil-off gas (BOG) from the cargo compressor. The pressurized BOG (~5 barg, 45°C) is re-condensed and mixed with LNG before entering the high-pressure (HP) booster pumps (90–130 barg). Thereafter, the LNG is vaporized at the vaporization train and exported through the export pipeline of the HP (High Pressure) manifold (Songhurst, 2017).

1.2 Module section

The process module and the control bridge of FSRU are located on the upper deck. Moreover, the equipment for each process is built as a separate module (**Table S2**) and retrofitted onto the tanker to reduce the time required for building a new FSRU. However, this module arrangement is limited by the hull connection and separation distance. Thus, the layout optimization of this study considered the process modules installed in the upper deck. In addition, the configuration and size (**Table S3**) of the module in the FSRU were selected to conform the construction track record.

1.3 Safety section

1.3.1 Quantitative risk assessment The risk involved in the FSRU operation was quantified by conducting the QRA to evaluate the probabilities of the identified hazardous events and their consequences based on historical data or frequency-modeling techniques. The QRA consists of (1) system definition, (2) hazard identification, (3) frequency and consequence analysis, and (4) individual risk analysis (Spouge, 1999).

(1) System definition

As discussed earlier, the QRA considered the process modules installed in the upper deck. The process module and the control bridge of FSRU are located on the upper deck. The power generation engine and utility system are on the hull deck. In this study, the module configuration of the hull deck was simply compared to the upper deck module, and thus excluded from QRA analysis.

(2) Hazard identification

This process involved identifying the dangerous components of the FSRU that could cause accidents and potentially escalate to affect the entire facility. The most probable accidents in the FSRU result from leakages (Paltrinieri *et al.*, 2015). LNG or NG can leak from pipes, flanges, valves, and process equipment of FSRU modules. In general, leakage scenarios can be established in two steps.

First, the isolatable sections should be defined; these are bounded by process shutdown valves (PSDVs) and are further divided into sub-isolatable sections based on different

compositions, phases, locations, and operating conditions (**Table S4**). Subsequently, all the identified hazards were categorized according to the leakage characteristic. In this study, four leakage scenarios were considered: small LNG leaks, medium LNG leaks, large LNG leaks, and LNG leaks caused by line rupture.

- Small leak (diameter D≤10 mm)
- Medium leak (10 mm<D≤50 mm)
- Large leak (50 mm<D≤150 mm)
- Line rupture (150 mm<D)

The identified hazards were used in the frequency analysis and consequence analysis to evaluate the probable accidents and the potential amount of damage they can cause.

In this study, fire and explosion scenarios were considered as outcomes of the LNG/NG leaks. The International Code for the construction and Equipment of Ships Carrying Liquefied Gases in Bulk (IGC Code) requires fire and explosion risk assessment at the design phase when a ship is operated at a fixed location in a re-gasification and gas-discharge mode or a gas receiving, processing, liquefaction, and storage mode for a period (No, 2014). In contrast, other events caused by LNG/LG leaks such as cryogenic damage and asphyxiation, can be avoided and mitigated by design improvement (low-temperature design, ventilation) (Bain *et al.*, 2006).

(3) Frequency analysis

The frequency of accidents can be calculated from historical data using a multiple-accidents modeling approach. In this study, the event-tree analysis (ETA) was applied to identify all the potential accident scenarios and sequences in the complex FSRU system (**Figure S1**). ETA is an inductive procedure that illustrates all the possible outcomes of an initiating event, considering the probability of ignition and the installed safety barriers are functioning appropriately.

(4) Consequence analysis

In parallel with the frequency analysis, consequence analysis was used to evaluate the consequences of the accidents. The consequence likelihood of a particular event can be estimated using several modeling approaches such as physical and phenomenal models and computational fluid dynamics (CFD) models (Spouge, 1999). In general, the most probable case of accident in LNG processes are flash fire, pool fire, jet fire, boiling liquid expanding vapor explosion, and vapor cloud explosion (Martins *et al.*, 2016).

In this study, the consequences of accidents were evaluated using known empirical models that can determine the quantity of thermal radiation or overpressure resulting from an accident (Freeman, 1990). In addition, several empirical models can be used for consequence analysis for each type of accident such as vapor cloud explosion (VCE), fireball, flash fire, or boiling liquid expanding vapor explosion. Furthermore, the probit analysis expressed in Eq. (1) was applied to obtain the probability P of fatality in Eq. (2).

$$Pr = k_1 + k_2 \ln V \tag{1}$$

$$P = 50\left[1 + \frac{Pr-5}{|Pr-5|} erf\left(\frac{|Pr-5|}{\sqrt{2}}\right)\right] \tag{2}$$

P can be determined by evaluation of Pr on a probit transformation chart, where k_1 and k_2 are the probit constants and V is the product of intensity or the concentration of the hazardous agent received to a component (Hewlett, 1972).

(5) Individual risk

The estimated frequencies and consequences of each modeled event have been estimated, they can be combined to form measures of the overall risk. Individual risk (IR) is the risk to a person who is near the hazard.

IR considers the nature, likelihood, and the time of a possible injury to an individual. One of the methods to obtain IR from the frequency and consequence analysis was suggested by the State of Sao Paulo Environmental Company, and the P4.261 standard establishes guidelines for estimating the risk and specifying the tolerability criteria (Martins *et al.*, 2016).

Here, a simplified expression of IR calculation is presented as Eq. (3), which assumes the weather and wind direction-independent effects of an accident. Therefore IR is the product of the frequency of the possible event (e.g., fire and explosion) and the probability of fatality by the event (Han *et al.*, 2013).

$$IR_{u,v} = \sum_i f_{eo,v} p_{u,v}^{fat} \tag{3}$$

The IR limit suggests the acceptable criterion, which is not an absolute standard but reasonably practicable according to the situation (Dan *et al.*, 2015). The newly-introduced FSRU requires high pressure and cryogenic operating conditions; in such as environment, the IR should be maintained at $<10^{-6}$ per year (Martins *et al.*, 2016) (**Table S5**).

In addition, IRs were affected by the distances from the centers of the process equipment. For this case study, the criteria of IR were tightened to $<10^{-6}$ (**Table 1**).

1.3.2 Noise The noise constraints are intended to prevent the occurrence of potentially hazardous noise levels on board ships and provide standards for an acceptable environment for the crew. These standards were developed to address passenger and cargo ships. In this study, the permissible noise level in the control room and the maximum permitted noise level in each module were applied (IMO, 2012).

The intensity from a point source of sound obeys the inverse-square law when reflections or reverberation are

Table 1 Safety distance required as per IR estimation

Section	Safety distance ($IR<10^{-6}$/y)	Remark
HP Vent Mast	2	
LNG Vent Mast	5	
Suction Drum	7	Case 3, 4
ReGAS	51	
Cargo Comp	4	
Liquid Dome	17	
Gas Dome	0	
HP Manifold	18	
LP Manifold	17	
MSO Comp	4	Case 2, 4

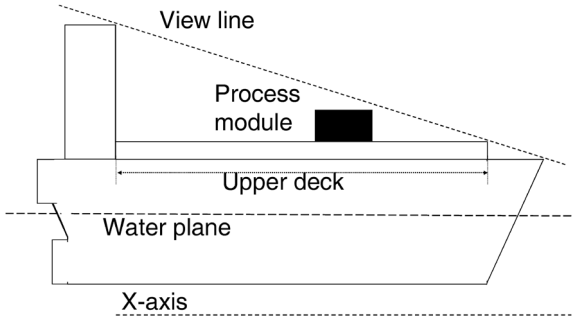

Fig. 5 FSRU view line

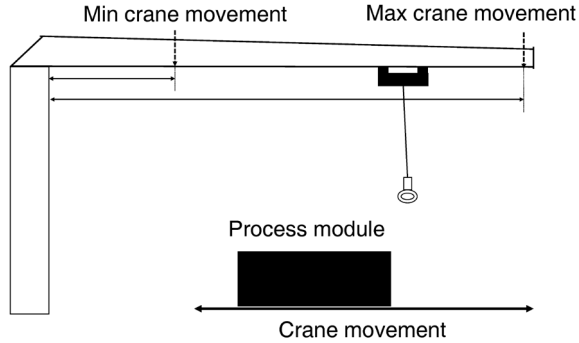

Fig. 6 Crane movement

Table 2 Safety distance required as per noise estimation

Module	Noise limit [dBA]	Safety distance [m]
Cargo compressor room	110	90 (dBA) : 10
		85 (dBA) : 18
		75 (dBA) : 56
ReGAS (Regasification)	90	85 (dBA) : 1.8
MSO compressor		75 (dBA) : 5.6
HP vent mast	85	75 (dBA) : 3.2
LNG vent mast 1/2/3/4		
Liquid dome 1/2/3/4		
Gas dome 1/2/3/4		
Suction drum		
HP manifold		
LP manifold 1/2		
Crane		
Control bridge	75	—

absent. The inverse square law can be expressed as Eqs. (4), (5) (Nave, 2000).

$$dL = L_{p2} - L_{p1} \tag{4}$$

$$d = L = 10\log\left(\frac{R_2}{R_1}\right)^2 \tag{5}$$

The required safety distances were calculated by defining the noise criteria for each module to satisfy the noise requirements (**Table 2**).

1.4 Operation and maintenance section

1.4.1 Visibility for vessel operation The risk of a collision has always accompanied marine transport. Despite improved navigation equipment, collision risk is currently greater because of the growing number of big fast-moving vessels. Thus, LNG vessels with the keel laid on or commissioned after 1 July 1998 must fulfill strict requirements regarding the visibility from the navigation bridge (Cairns, 2011) (**Figure 5**). As sufficient visibility must be maintained for the ship operation, the height of each module is restricted for visibility.

1.4.2 Crane for maintenance In FSRUs, a crane is required to re-install and repair individual equipment in the module. Thus, the distance from the process module should be within the distance available to the crane hook (**Figure 6**).

2. Model Formulation

2.1 Mathematical approach for layout optimization

The mathematical model of the FSRU layout optimization will be presented as mixed-integer linear programming (MILP) and solved in general algebraic modeling system (GAMS) with the CPLEX solver to minimize the total pipeline cost of the FSRU.

$$\min\ obj = \text{total pipeline connection cost}$$

$$\text{s.t.}\ \left.\begin{array}{l} h(y,Y) = 0 \\ g(y,Y) \geq 0 \end{array}\right\} \left\{\begin{array}{l} \text{Dimension and orientation} \\ \quad \text{of equipment} \\ \text{Area limiation constraints} \\ \text{Non-overlapping of} \\ \quad \text{equipment constraints} \\ \text{Process boundary constraints} \\ \text{Safety distance constraints} \\ \text{Crane movement constraints} \\ \text{Hull arrangement limits} \\ \text{Noise limits} \\ \text{Visibility constraints} \end{array}\right.$$

$$y \in \mathbb{R},\ Y \in \{0,1\}$$

Where y and Y are vectors of continuous and binary variables, respectively.

The objective function of the FSRU layout optimization problem is to minimize the total pipeline cost between the modules in FSRU, as expressed in Eq. (6).

$$\min \sum_i \sum_{j \neq i} C_{ij}^{\text{pipe}} TD_{ij} \tag{6}$$

The pipeline connection cost is the unit cost of the pipeline multiplied by the rectilinear distance between the connected equipment (Xu and Papageorgiou, 2009). The rectilinear distance maintains the linearity of the problem and represents the actual pipeline connections in the process industry. Each type of pipe has a specific cost per unit length (**Table S6**).

2.2 Dimension and orientation of equipment

This analysis considered the area occupied by the equipment and the spacing between the equipment. The rectangular equipment was located either horizontally or vertically, as expressed in Eqs. (7), (8) with the binary variable O_i.

$$l_i = a_i O_i + b_i(1-O_i) \qquad \forall i \tag{7}$$

$$d_i = a_i + b_i - l_i \qquad \forall i \tag{8}$$

The distance between each equipment can be defined using binary variables W_{ij}^x and W_{ij}^y. Eqs. (11)–(14) express that the equipment cannot be placed both on the right and left or above and below of other equipment.

$$R_{ij} - L_{ij} = x_i - x_j \quad \forall i = 1 \ldots N-1, \quad \forall j = i+1, \ldots N \tag{9}$$

$$A_{ij} - B_{ij} = y_i - y_j \quad \forall i = 1 \ldots N-1, \quad \forall j = i+1, \ldots N \tag{10}$$

$$R_{ij} \le M W_{ij}^x \quad \forall i = 1 \ldots N-1, \quad \forall j = i+1, \ldots N \tag{11}$$

$$L_{ij} \le M(1 - W_{ij}^x) \quad \forall i = 1 \ldots N-1, \quad \forall j = i+1, \ldots N \tag{12}$$

$$A_{ij} \le M W_{ij}^y \quad \forall i = 1 \ldots N-1, \quad \forall j = i+1, \ldots N \tag{13}$$

$$B_{ij} \le M(1 - W_{ij}^y) \quad \forall i = 1 \ldots N-1, \quad \forall j = i+1, \ldots N \tag{14}$$

$$TD_{ij} = R_{ij} + L_{ij} + A_{ij} + B_{ij} \tag{15}$$

$$\forall i = 1, \ldots, N-1, \quad \forall j = i+1, \ldots, NA$$

In case an equipment i is on the right-hand side of j, the horizontal distance between their centers in a two-dimensional plane is R_{ij}. When i is on the left of j, the distance is L_{ij}. Similarly, the vertical distances were defined as A_{ij} (above) or B_{ij} (below). The total distance is expressed in Eq. (15).

2.3 Dimension and orientation of equipment

Modules and equipment cannot be placed in the "fore peripheral" or "after peripheral" areas of the FSRU (**Figure 7**).

The module placement must be configured in the length between peripherals (LBP). The width and LBP of the FSRU were modeled under the modular placement limit in Eqs. (16), (17).

$$LBP \cdot O_i + WD(1-O_i) = x^{\max} \qquad \forall i \tag{16}$$

$$LBP - WD - x^{\max} = y^{\max} \tag{17}$$

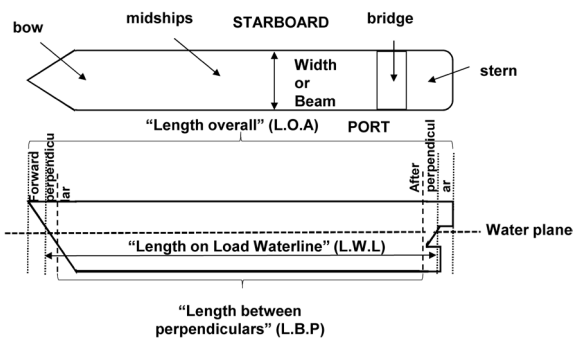

Fig. 7 Ship Dimensions (Schematic)

2.4 Non-overlapping constrains

The basic non-overlapping constraints using big-M are as follows in Eqs. (18)–(21) (Park *et al.*, 2018a).

$$x_i - x_j + M(E1_{ij} + E2_{ij}) \ge \frac{l_i + l_j}{2} \tag{18}$$

$$x_j - x_i + M(1 - E1_{ij} + E2_{ij}) \ge \frac{l_i + l_j}{2} \tag{19}$$

$$y_i - y_j + M(1 + E1_{ij} - E2_{ij}) \ge \frac{d_i + d_j}{2} \tag{20}$$

$$y_j - y_i + M(2 - E1_{ij} - E2_{ij}) \ge \frac{d_i + d_j}{2} \tag{21}$$

$$\forall i = 1, \ldots, N-1, \forall j = i+1, \ldots, N$$

$E1_{ij}$ and $E2_{ij}$ are binary variables that control the application of Eqs. (18)–(21) along with an appropriately large number M. In addition, Eq. (18) is active when $E1_{ij}$ and $E2_{ij}$ are both zero, otherwise it is redundant. Similarly, Eq. (19) is active only if $E1_{ij} = 1$ and $E2_{ij}$ 0, Eq. (20) is active only if $E1_{ij} = 0$ and $E2_{ij} = 1$, and Eq. (21) is active only if $E1_{ij} = E2_{ij} = 1$. These constraints cause the distance between the two equipment to be greater than or equal to the sum of half of the length of their sides on both axes.

2.5 Process boundary constrains

The process equipment should be placed within a constrained area, and the restriction at the center of the equipment within the boundary can be modified to model this zone. The basic boundary conditions are as follows in Eqs. (22)–(25).

$$x_i \ge \frac{l_i}{2} \qquad \forall i \tag{22}$$

$$y_i \ge \frac{d_i}{2} \qquad \forall i \tag{23}$$

$$x_i + \frac{l_i}{2} \le x^{\max} \qquad \forall i \tag{24}$$

$$y_i + \frac{d_i}{2} \le y^{\max} \qquad \forall i \tag{25}$$

The minimum distance from the boundary of the FSRU was maintained by adding BD and l (d) in Eqs. (26), (27).

$$x_i + \frac{l_i}{2} \ge BD_i \qquad \forall i \tag{26}$$

$$y_i + \frac{d_i}{2} \ge BD_i \qquad \forall i \tag{27}$$

The manifold should be installed at the boundary of FSRU to facilitate the connection with LNG carrier or onshore terminal, and other modules should be separated from the vessel boundary (**Table 3**).

2.6 Safety distance constrains

The safety distance calculated from the results of the QRA IR differed among the modules. At least one of the horizontal or vertical distances between the control room and equipment should be greater than or equal to the sum of the spacing for

Table 3 Boundary distances according to the module types

Module type	Boundary distance [m]
Control room	2
Engine casing	2
Process module	2
Cargo tank module (Liquid dome, Gas dome)	2
Vent mast	2
LP/HP manifold	0
Crane	2

workers and half the length of their sides in Eqs. (28)–(30).

$$R_{ij} + L_{ij} \geq SD_j + \frac{l_i}{2} + \frac{l_j}{2} - M \cdot Swv1_i \tag{28}$$
$$\forall i \neq \text{ctrl room}, \forall j = \text{ctrl room}$$

$$A_{ij} + B_{ij} \geq SD_j + \frac{d_i}{2} + \frac{d_j}{2} - M \cdot Swv2_i \tag{29}$$
$$\forall i \neq \text{ctrl room}, \forall j = \text{ctrl room}$$

$$Swv1_i + Swv2_i \leq 1 \tag{30}$$
$$\forall i \neq \text{ctrl room}, \forall j = \text{ctrl room}$$

2.7 Crane movement constrains

The crane moves the equipment inside the cargo compressor room and equipment from the process module to enable maintenance of the FSRU equipment. The distance from the process module must be less than the maximum range $CMS_i^{\max}$ of the crane hook because the cranes must be located within the range within which the equipment can be moved in the module. Moreover, cranes cover a minimum distance $CMD_i^{\min}$ to reach each module (Figure 6).

$$R_{ij} + L_{ij} + A_{ij} + B_{ij} \leq M(1 - Cwv1_{ij}) + CMD_j^{\max} \tag{31}$$
$$\forall i \notin \{\text{crane}\}, j \in \{\text{crane}\}$$

$$R_{ij} + L_{ij} + A_{ij} + B_{ij} \geq M \cdot Cwv1_{ij} + CMD_j^{\max} \tag{32}$$
$$\forall i \notin \{\text{crane}\}, j \in \{\text{crane}\}$$

$$CMD_j^{\min} - (R_{ij} + L_{ij} + A_{ij} + B_{ij}) \leq M(1 - Cwv2_{ij}) \tag{33}$$
$$\forall i \notin \{\text{crane}\}, j \in \{\text{crane}\}$$

$$R_{ij} + L_{ij} + A_{ij} + B_{ij} - CMD_j^{\min} - \leq M \cdot Cwv2_{ij} \tag{34}$$
$$\forall i \notin \{\text{crane}\}, j \in \{\text{crane}\}$$

$$Cwv1_{ij} + Cwv2_{ij} - 1 \leq Cwv_{ij} \leq \frac{Cwv1_{ij} + Cwv2_{ij}}{2} \tag{35}$$
$$\forall i \notin \{\text{crane}\}, j \in \{\text{crane}\}$$

$$\sum_{j \in \text{crane}} Cwv_{ij} \geq 1 \quad \forall i \notin \{\text{crane}\} \tag{36}$$

2.8 Hull arrangement limit for LNG tank

The LNG tank process module was connected to the submerged LNG pump of the hull deck. The layout of the LNG tank gas/liquid dome and LP vent mast was not free outside the tank area. To comply with the arrangement limit of LNG tanks, an appropriate distance is required between the gas/liquid domes following the inequality constraints in Eqs. (37), (38) (**Table S7**).

$$R_{ij} + L_{ij} \geq HSD_{ij} + \frac{l_i}{2} + \frac{l_j}{2} \tag{37}$$
$$\forall i \notin \text{gas, liquid dome, lng vent mast},$$
$$j \in \text{gas, liquid dome, lng vent mast}$$

$$A_{ij} + B_{ij} \geq HSD_{ij} + \frac{d_i}{2} + \frac{d_j}{2} \tag{38}$$
$$\forall i \notin \text{gas, liquid dome, lng vent mast},$$
$$j \in \text{gas, liquid dome, lng vent mast}$$

2.9 Module spacing limit

The manifold modules for unloading and loading must be located at a minimum distance from the module to provide a certain clearance during installation between the modules. Therefore, an appropriate equipment spacing is required as an inequality constraint. That can be constructed by simply adding it is constructed simply by adding the spacing to the conventional 'dimension and orientation' constraints (**Table S8**).

$$R_{ij} + L_{ij} \geq MSD_i + MSD_j + \frac{l_i}{2} + \frac{l_j}{2} \qquad \forall i \ \forall j \tag{39}$$

$$A_{ij} + B_{ij} \geq MSD_i + MSD_j + \frac{d_i}{2} + \frac{d_j}{2} \qquad \forall i \ \forall j \tag{40}$$

2.10 Noise level limit constraints

The separation distance satisfying the noise standard between modules is defined in Eqs. (41)–(43).

$$R_{ij} + L_{ij} \geq SND_j + \frac{1_i}{2} + \frac{1_j}{2} - M \cdot Nwv1_{ij} \qquad \forall i, \forall j \tag{41}$$

$$A_{ij} + B_{ij} \geq SND_j + \frac{d_i}{2} + \frac{d_j}{2} - M \cdot Nwv2_{ij} \qquad \forall i, \forall j \tag{42}$$

$$Nwv1_{ij} + Nwv2_{ij} \leq 1 \qquad \forall i, \forall j \tag{43}$$

2.11 Visibility constraints

Adequate visibility must be available for the operation of the ship (Figure 5). The layout of each module is restricted under visibility, and tall modules must be located under the view line. In addition, each module must be placed within an unobtrusive range of view line the height γ_i of i should not exceed the view line and that is assumed to be a linear function of x_i in Eq. (44).

$$\gamma_i \leq -V_1 \cdot x_i + V_2 \qquad \forall i \neq \text{Ctrl Bridge} \tag{44}$$

3. Case Study

Four configurations of FSRU were examined to evaluate the influence of separating modules and the inclusion of

additional modules (**Table 4**) (**Figures S2–S5**). The process configuration of FSRU could be influenced by the minimum send-out capacity and the regasification module design.

The minimum send-out capacity of the FSRU was determined using the minimum booster pump capacity, which was assumed as 50 MMSCFD in this study. If the onshore terminal requires a small amount (~5 t/h) of send out that is less than the minimum capacity of the booster pump, then an additional minimum send-out (MSO) compressor with low capacity (5 t/h) and high pressure (~100 barg) is required for Case 2 and Case 4.

A suction drum was typically included in the regasification module of the FSRU. The size and weight of the regasification module was reduced for easy installation by considering suction drums that were manufactured as separate modules for Case 3 and Case 4. In all the cases, the LNG tank and the LP/HP manifold were installed in common.

4. Results and Discussion

Four case studies were conducted to determine influence of module separation (**Table 5**). The piping cost increased with the number of modules in the FSRU.

A majority of the modules were connected to the LP manifold, and the connected piping costs accounted for 46–48% of the total piping cost (**Figure 8**). The LP manifold was placed mainly in the middle section of the vessel; thus, the position of the LP manifold remained unchanged for Cases 1–4.

Each set of liquid dome and gas dome should be installed on the top of the LNG tank and connected with the corresponding LNG tank using multiple piping. The total piping cost of each set of the liquid, gas dome and LP manifold was minimized by assuming that the single coordinate of the liquid/gas dome, and LP manifold module were identical on the upper deck. In addition, the LNG vent mast was placed to avert overpressure accumulation inside the Liquid Dome and satisfy the minimum separation distance (2 m) for all cases (**Figure 9**).

The separation effect of the regasification module was further investigated. As compared with Case 1 and Case 2, the regasification module in Case 3 and Case 4 assumed to be separated with the suction drum module. The case studies demonstrated that the piping cost for the regasification module increased by ~USD 60,000 in Cases 3 and 4, whereas the other piping costs decreased (Figure 8).

Regardless of the separation of regasification modules, the piping for connecting with the regasification module is expensive (US$ 1000/m), so the HP manifold should be placed close to the regasification module in all the cases.

The MSO compressor tends to be placed near the cargo compressor room in both Cases 2 and 4, because the suction piping cost (US$ 350/m) associated with the cargo compressor room is higher than the discharge piping cost (US$ 170/m) associated with the HP manifold. Although

Table 4 FSRU process configurations of upper deck module

Case	FSRU process configuration
1	Base model
2	MSO compressor is installed if minimum NG send-out capacity is ~5 t/h
3	The suction drum is separately installed to reduce regasification module weight and complexity
4	Adding an MSO compressor + separating a suction drum

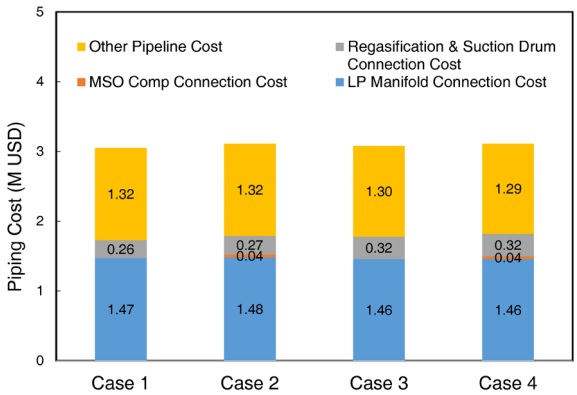

Fig. 8 The pipe connection cost ratio for Case 1–4

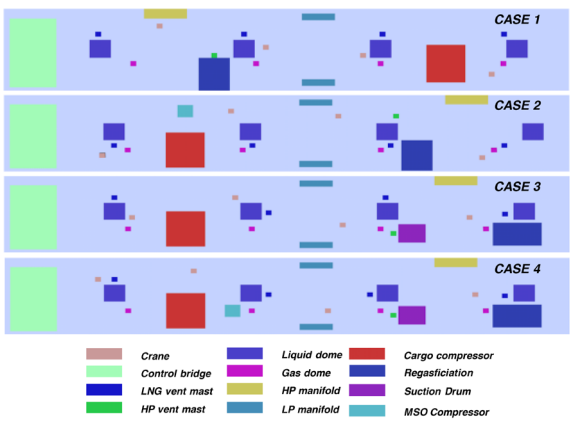

Fig. 9 FSRU 2D layout (Case 1–4)

Table 5 Pipeline cost estimation by layout optimization

Case	Num. of modules	FSRU module configuration	Total pipe length [m]	Total cost [$10^6$$]	Cost compared to Case 1
1	23	Regasification + cargo comp.	4,290	3.052	
2	24	Regasification + cargo comp. + MSO comp.	4,634	3.110	101.9%
3	24	Suction drum + regasification + cargo comp.	4,408	3.081	101.0%
4	25	Suction drum + regasification + cargo comp. + MSO comp.	4,620	3.113	102.0%

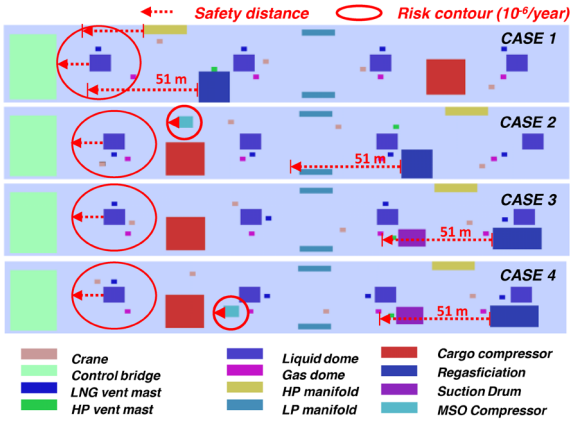

Fig. 10 FSRU layout with risk contour (Case 1–4)

the MSO Compressor is located in vicinity of the cargo compressor room, the distance between the two modules is about 10 m. Moreover, the MSO compressor must be placed 10 m away from the cargo compressor room (125 dBA) to satisfy the noise criteria (90 dBA).

Three number of modules were connected to the MSO compressor (cargo compressor room, HP manifold, HP vent mast). Therefore, the proportion of the piping cost related to MSO compressor accounts to only 1.3% and does not significantly affect the overall piping cost (Figure 8).

Moreover, IR contour was suggested to estimate the fire and explosion risk toward the control bridge. In addition, the control bridge was placed on the corner of the upper deck to secure a safety distance from the process modules (Cases 1–4) (**Figure 10**).

Furthermore, we compared the cases to check the differences in the separation of regasification modules. The position of the regasification module in cases 3 and 4 was shifted to the farthest point from the control bridge as compared to that in Cases 1 and 2 (Figure 10).

Although the regasification module was separated, the safety distance (51 m) requirement was still constant as this module exhibited the highest individual risk owing to its high pressure (100 barg) operating condition and large capacity (750 MMSCFD).

Although the MSO Compressor and HP Manifold are generally operated at high pressures, their risk contours are smaller than that of the regasification module (Figure 10). As the operation capacity of a MSO compressor is extremely small (5 t/h), the effect of explosion is not large, and the piping configuration of the HP manifold is simple, so the leakage frequency is very low.

In addition, the cranes were uniformly placed on the upper deck for maintenance, and the module was not placed in the inoperable area of the crane. An inspection of the ranges of crane operation determined that the number of cranes was adequate for maintenance. Moreover, the optimal positioning of the cranes for equipment installation and maintenance functions was secured inside the entire module (**Figures S6–S9**). The four cranes installed in the FSRU could be used for maintenance of modules on board and load/unload equipment from ship to ship or ship to shore (Cases 1–4).

The placement of the crane module was constrained by the location of a module closest to the minimum and maximum operating radii of the crane. Moreover, and analysis of the operation range of the crane demonstrated that its location was affected by the module closest to the minimum operation range in all cases. In particular, the gas dome and the LNG vent mast influenced the crane positioning.

In all the cases, the view line of the FSRU was set to not interfere with the sailing of the FSRU vessel (**Figures S10–S13**).

Furthermore, an integrated optimization model was developed for the layout design of a FSRU system to obtain the expected total piping cost. At the design stage, this method could estimate the initial cost of the pipeline installed in the upper deck. Thus, the total piping cost was only around 2% under various process configurations discussed in the case studies (Table 5). The selection of piping cost at ~102% of the initial estimate will provide flexibility to respond toward unanticipated scenarios.

The layout observed in the case studies could be used as an initial FSRU module layout to improve the design. Therefore, the use of optimization models for layout may be considered as a tool to help the engineer for selecting among a large number of possibilities (Guirardello and Swaney, 2005). The optimality of the layout design can be increased with the following directions recommended for further studies.

(1) A cost trade-off analysis should be conducted to determine the economically optimal layout option, considering piping cost and module internal piping/construction cost.
(2) An optimization study should be conducted using advanced numerical formulation to define the minimum number of cranes and the corresponding cost.
(3) A 3D layout optimization technique is required with additional constraints to prevent the interference of pipe path and module positions.
(4) Unnecessary or overlapping piping connections can be minimized using layout optimization for all node positions.

Conclusions

This research developed a new framework of module layout optimization using a quantitative assessment of individual risk for process modules and operation and maintenance management. We presented the layout optimization problem for FSRU design, considering risk, operation, and maintenance. In addition, the process module was modeled using distance constraints and design rules. The proposed layout suggested guidelines to design the layout of FSRU considering various distance measures, including module_module distance, control room-module distance and module_boundary distance.

The case studies demonstrated that the proposed method

was effective in obtaining an optimized FSRU layout along with the required piping cost under various process configurations. The required number of cranes for maintenance and crane operating range verification was inspected from the layout results for each case. Moreover, the case studies presented the risk contour and safety distance requirement for each process module by considering the results of fire and explosion risk assessment.

The proposed approach could be improved in certain ways such as using multi-objective optimization for the modules, piping and crane cost, three-dimensional numerical modeling for detailed pipe routing configuration, and including the pipe and module weight. These issues will be addressed in future research.

Supplementary Information

Supplementary Information is available at http://www.scej.org/publication/jcej/suppl/

Literature Cited

Bain, B., M. Celnik and G. Korneliussen; "Practical Application of the UKOOA Ignition Model," Hazards XXIII. Sympoisum Series, Institution of Chemical Engineers, London, U.K. (2006)

Cairns, B.; "Navigation Bridge Visibility-SOLAS V/22," Bulletin de l'AISM (2011)

Dan, S., D. Shin and E. S. Yoon; "Layout Optimization of LNG-Liquefaction Process on LNG-FPSO Preventing Domino Effects," *J. Chem. Eng. Japan*, **48**, 646–655 (2015)

Ejeh, J. O., S. Liu and L. G. J. C. Papageorgiou; "Optimal Layout of Multi-Floor Process Plants Using MILP," *Comput. Chem. Eng.*, **131**, 106573 (2019)

Freeman, R. A.; "CCPS Guidelines for Chemical Process Quantitative Risk Analysis," *Plant. Oper. Prog.*, **9**, 231–235 (1990)

Georgiadis, M. C., G. Schilling, G. E. Rotstein, S. J. C. Macchietto and C. Engineering; "A General Mathematical Programming Approach for process plant Layout," *Comput. Chem. Eng.*, **23**, 823–840 (1999)

Giardina, M. and M. Morale; "Safety Study of an LNG Regasification Plant Using an FMECA and HAZOP Integrated Methodology," *J. Loss. Prevent. Proc.*, **35**, 35–45 (2015)

Guirardello, R. and R. E. J. C. Swaney; "Optimization of Process Plant Layout with Pipe Routing," *Comput. Chem. Eng.*, **30**, 99–114 (2005)

Han, K., Y. H. Kim, N. Jang, H. Kim, D. Shin and E. S. Yoon; "Risk Index Approach for the Optimal Layout of Chemical Processes Minimizing Risk to Humans," *Ind. Eng. Chem. Res.*, **52**, 7274–7281 (2013)

Hewlett, P.; "Probit Analysis" D. J. Finney ed., Cambridge University Press, Cambridge, U.K. (1972)

IMO; Code on Noise Levels on Board Ships, The Maritime Safety Committee, London, U.K. (2012)

Jeong, S.-Y., M.-I. Roh and H. Shin; "Multi-Floor Layout Model for Topsides of Floating Offshore Plant using the Optimization Technique," *J. Soc. Nav. Archit.*, **52**, 77–87 (2015)

Kobayashi, K.; "New Concept for Standardized Large-Scale Modular LNG Plant Design," *LNG 19* (2019)

Ku, N.-K., J.-H. Hwang, J.-C. Lee, M.-I. Roh, K.-Y. J. S. Lee and O. Structures; "Optimal Module Layout for a Generic Offshore LNG Liquefaction Process of LNG-FPSO," *Ships Offshore Struct.*, **9**, 311–332 (2014)

Maksyma, K. and D. A. Wood; "Floating Storage and Regasification Units Face Specific LNG Rollover Challenges: Consideration of Saturated Vapor Pressure Provides Insight and Mitigation Options," *N.G.I.B.*, **5**, 391–414 (2018)

Martins, M. R., M. Pestana, G. Souza and A. Schleder; "Quantitative Risk Analysis of Loading and Offloading Liquefied Natural Gas (LNG) on a Floating Storage and Regasification Unit (FSRU)," *J. Loss Prev. Process Ind.*, **43**, 629–653 (2016)

Nave, R.; Hyper Physics, Georgia State University, Department of Physics and Astronomy, Atlanta, U.S.A. (2000)

No, T. S.; "International Code for the Construction and Equipment of Ships Carrying Liquefied Gases in Bulk (IGC Code)," International Maritime Organization, London, U.K. (2014)

Paltrinieri, N., A. Tugnoli and V. Cozzani; "Hazard Identification for Innovative LNG Regasification Technologies," *Reliab. Eng. Syst. Saf.*, **137**, 18–28 (2015)

Papageorgiou, L. G. and G. E. J. I. Rotstein; "Continuous-Domain Mathematical Models for Optimal Process Plant Layout," *Ind. Eng. Chem. Res.*, **37**, 3631–3639 (1998)

Park, K., D. Shin and W. Won; "Risk Based 3-Dimensional and Multifloor Plant Layout Optimization for Liquefied Natural Gas (LNG) Liquefaction Process," *Korean J. Chem. Eng.*, **35**, 1053–1064 (2018a)

Park, S., B. Jeong, B. S. Lee, S. Oterkus and P. J. O. E. Zhou; "Potential Risk of Vapour Cloud Explosion in FLNG Liquefaction Modules," *Ocean Eng.*, **149**, 423–437 (2018b)

Park, S., S. Kim, Y. Yoon, I.-B. Lee and E. S. Jung; "A Comparative Evaluation of Heating Method Options for Floating Storage Regasification Units Using Life Cycle Cost Analysis with Risk Expenditure," *J. Chem. Eng. Japan*, **52**, 751–765 (2019)

Patsiatzis, D., G. Knight and L. J. C. E. R. Papageorgiou; "An MILP Approach to Safe Process Plant Layout," *Chem. Eng. Res. Des.*, **82**, 579–586 (2004)

Songhurst, B.; "The Outlook for Floating Storage and Regasification Units (FSRUs)," Oxford Institute for Energy Studies, Oxford, U.K. (2017)

Spouge, J.; A Guide to Quantitative Risk Assessment for Offshore Installations, CMPT, Aberdeen, U.K. (1999)

Xu, G. and L. G. Papageorgiou; "Process Plant Layout Using an Improvement-Type Algorithm," *Chem. Eng. Res. Des.*, **87**, 780–788 (2009)